

sequences) with a cut-off *E*-value of 10^{-4} . If the sequence identity and the coverage between a sequence hit and the human were higher than 40% and 80%, respectively, the sequence was selected as a homologous sequence. When two or more sequences from an organism were found as homologous sequences, the sequence with the highest sequence identity was only considered. The homologous protein sequences from various organisms were aligned using the CLUSTAL W program.³⁶ A degree of sequence conservation at each amino acid position in the multiple sequence alignment (simply designated as 'residue conservation' in Fig. 1) was defined as the ratio of (the number of the homologous protein sequences which carried an identical amino acid residue to that in the human sequence) to (the number of the aligned homologous protein sequences) at the specified position in the multiple sequence alignment. For example, if Ala appears in an aligned position in the human sequence and the corresponding positions in all of the other homologous sequences are also Ala, the residue conservation in this position is defined as 1.0. The frequency distribution of the residue conservations in disease-associated missense mutation or nsSNP positions for proteins analysed in this study was represented using bins of the interval of 0.2. The value in each bin was normalized by the frequency of the total number of residues in each bin.

2.3. Protein 3D structure information

Protein 3D structure data were downloaded from the Protein Data Bank (PDB, <http://www.rcsb.org/pdb/>).³⁷ In cases where the 3D structure of a human protein had not yet been determined, we

searched the available sequences in the PDB entries for a template structure for homology modelling using the BLAST program as described above. When the alignment of the human protein sequence and a known 3D structure showed >30% identity and >90% coverage, a homology model was built using the MODELLER package.³⁸ For each target, 20 model structures were generated and their reliabilities were assessed with the Discrete Optimized Protein Energy (DOPE) method.³⁹ Eventually, the model with the best DOPE score was selected as the final model for each protein. Information about protein quaternary structures was also extracted from the PDB database. Entries from the PDB that contained information about the biological unit structure and entries with polypeptide chains showed >85% identities with a human protein sequence were considered. When a distance of one atom in a residue in a given polypeptide chain was <5.0 Å from that of another residue in the other polypeptide or nucleotide chain, the residue was considered to be located at a molecular interaction interface.

2.4. Solvent accessibility calculations

The solvent accessibilities of the amino acid residues in a 3D modelled structure were calculated using a modification of the Shrake and Rupley method,⁴⁰ with a water molecule represented by a 1.4 Å radius sphere. The solvent accessibility is represented by values ranging from 0 to 1. The residue was considered as an exposed residue on the protein surface, if the solvent accessibility was >0.25 and buried otherwise.

2.5. Disorder prediction

We used the DISOPRED2 program⁴¹ to analyse each amino acid sequence of a gene product and predict intrinsically unstructured (disordered) regions in the protein sequence. If the program predicted a region consisting of more than three amino acid residues in a sequence to be 'disordered', we assigned this region as an intrinsically unstructured one.

2.6. Predicting the effect of ns substitutions on proteins

The effects of ns substitutions on a given protein were evaluated on a local server using the SIFT program²⁶ which predicts the effects of missense substitutions on a protein based on evolutionary information from homologous protein sequences.

2.7. System implementation

At the server end, a set of common gateway interface programs was written in Perl and is running on an Apache web server. The information regarding the disease-associated genes and the sequence variations

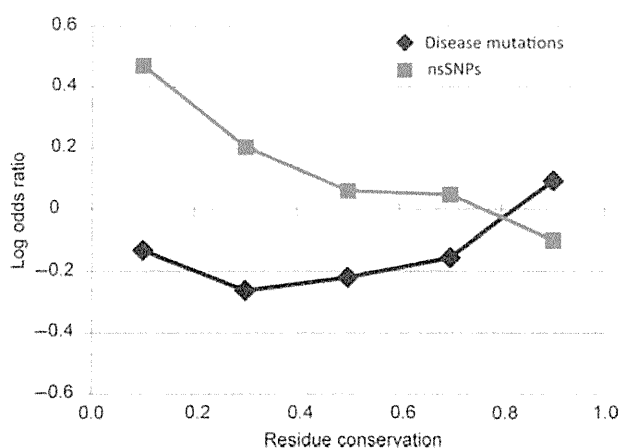


Figure 1. Comparison of frequency distributions of residue conservations in disease-associated missense mutations and nsSNPs. The vertical axis depicts the log-odds ratio of the frequency of ns substitution residue positions (disease-associated mutations or nsSNPs) to those of total number of residues in each residue conservation bin.

described above was integrated into a MySQL database implemented in the server. At the client end, JavaScript frameworks such as prototype.js (<http://www.prototypejs.org/>) and scriptaculous.js (<http://script.aculo.us/>) were used to make the user interface more interactive. Jmol, a Java applet (<http://www.jmol.org/>), was implemented for visualizing protein 3D structures in a web browser.

3. Results and discussion

3.1. Statistics of the sequence variation data on Mutation@A Glance

From three data resources for human disease mutations, OMIM, UniProt and RAPID, we obtained 25 616 disease-associated mutations and 21 199 nsSNPs in 2656 human genes (Table 1) and integrated into the local database. Functional classification of the proteins encoded by the disease-associated genes showed a wide variety of molecular functions such as metabolic enzymes, protein kinases, transcription factor/regulators and structural proteins (Table 1 and Supplementary Table S1). Because we have been actively analysing mutations found in patients of PIDs with paediatricians in Japan, we constructed RAPID and used it as our original data resource for genetic variations in genes responsible for PIDs.¹⁷ RAPID contains manually curated mutation data from published literature, including nonsense (582 sites in 96 genes), frameshift (851 sites in 101 genes) and insertion/deletion (85 sites in 42 genes) mutations as well as missense mutations (1564 sites in 116 genes) in the protein-coding regions of 155 PID genes (as of August 2009). For non-PID genes, we used two publicly available data sets from UniProt and OMIM. The UniProt database contains only missense mutation data (22 258 entries in 2614 genes). On the other hand, the OMIM database contains a large number of missense mutation (1899 entries in 556 genes) and a relatively small number of the other types of mutations (99 entries in 13 genes). The RAPID and the OMIM databases also contain 699 disease-associated mutation data in intronic regions of 147 genes that cause splice anomaly effects. Thus, the most frequent mutation type in our data sets was missense mutation (89% of the total entry) as reported in the previous study.¹³

3.2. Evolutionary, structural and functional features of the ns substitution positions

In general, disease-associated missense mutations tend to occur at evolutionarily conserved positions, because these positions are usually essential for the structure and/or function of a protein.^{26,42,43} To

Table 1. Functional classification of disease-associated gene products

Molecular class	No. of genes	No. of mutations ^a	No. of nsSNPs
Enzymes	410	5406 (5003)	2476
Protein kinases	258	1947 (1340)	2452
Transcription factor/regulator	239	2889 (2743)	1502
Structural proteins	132	1588 (1377)	1800
Cell surface receptors	123	1271 (1165)	838
Transport/cargo protein	116	1617 (1411)	1139
DNA/RNA binding proteins	97	429 (369)	580
Integral membrane protein	87	446 (434)	698
Channels	79	958 (948)	639
GTPase/GTPase regulators	71	371 (351)	450
Membrane transport protein	67	755 (751)	523
Immunity proteins	58	496 (183)	423
Extracellular matrix protein	53	886 (884)	939
Proteases	53	345 (284)	368
Cell adhesion molecules	52	390 (363)	428
Others	430	4647 (4091)	3863
Unclassified	331	1175 (987)	2081
Total	2656	25 616 (22 684)	21 199

^aThe numbers in parentheses indicate the number of disease-associated missense mutations.

verify this using the up-dated data set, we compared the frequency of disease-associated missense mutation sites (19 128 unique positions in 2622 genes) in each residue conservation bin with that of nsSNP sites (20 605 positions in 2494 genes) (Fig. 1). The results indicated that the previously reported tendency was still true for the 2622 genes in our data set; the disease-associated mutation sites were preferably appeared in the highest residue conservation bin, while nsSNP sites showed the opposite trend (Fig. 1). Next, we cross-referenced amino acid positions of the disease-associated missense mutations and nsSNPs to the functional features and 3D structures of the protein data in Mutation@A Glance. We classified these positions in terms of their functional features in a protein (annotated in the UniProt databases; Table 2). More disease-associated missense mutations were found in the positions annotated to have some functional features, except in the 'signal peptides' and 'post-translational modification sites', than nsSNPs. Using a homology modelling technique, we mapped 10 939 out of 19 128

Table 2. Structural and functional loci of mutation/nsSNP sites

Property	Disease mutations	nsSNPs
Transmembrane helix	1283	648
Nucleotide binding	670	102
Disulfide bond	385	39
Metal binding site	226	147
Signal peptide	101	262
Post translational modification site	97	104
Binding site ^a	48	12
Active site ^a	25	6

^aAs defined in UniProt database (described in the text).

disease-associated mutation sites (57.2%) to protein 3D structures (Fig. 2). Of these sites, 6616 sites (60.4%) were located in regions buried in protein

structures (solvent accessibility <0.25). In the same way, 7106 out of 20 605 nsSNP sites (34.4%) were mapped to 3D structures, and 4258 sites (59.9%) were located on the surfaces of proteins (Fig. 2A). This observation is basically consistent with the previous findings from structural analysis.^{44–46} Interestingly, nsSNP sites were located in regions predicted as intrinsically disordered at a three times higher frequency than disease-associated mutation sites (Fig. 2A). This might be ascribed to the observation that conservation in the intrinsically disordered regions is relatively lower than that in ordered regions.⁴⁷

Proteins function with other molecules in molecular networks (e.g. signalling pathways) in many cases. Hence, the effects of mutations on molecular interactions must be intriguing in mutation

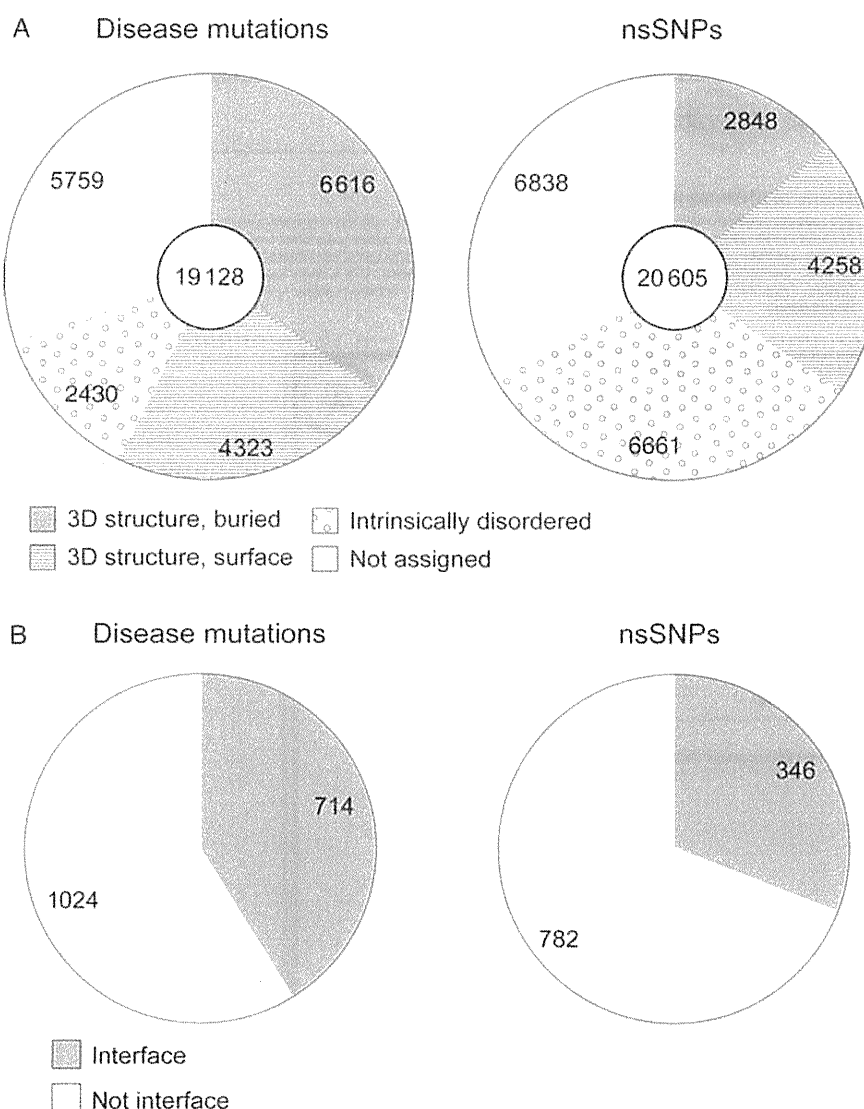


Figure 2. Classification of disease-associated mutations and nsSNPs according to their location on protein 3D structure. (A) The numbers in the pie charts depict those of ns substitution positions. (B) Proportion of ns substitution positions in the disease-associated mutations or nsSNPs that were located on the interface of the experimentally determined quaternary structures.

analysis.⁴⁸ We thus analysed whether or not the missense mutation positions were located in the molecular interaction sites based on the quaternary protein structures available from the PDB. Consequently, 714 out of 1738 disease-associated mutation sites (41.1%) were found to locate at the interfaces of 474 distinct proteins known to be involved in protein complex structures (Fig. 2B; see Section 2.3). In contrast, the same was true for only 346 out of 1128 nsSNP sites (30.7%) in 447 genes. We confirmed that the frequency of disease-associated mutation sites located at the molecular interaction interface was significantly higher than that of nsSNP sites by χ^2 test ($P < 0.01$). These results implicated that ns substitutions at positions involved in the molecular interaction tend to be disease-related as we expected.

3.3. The user interface for visualizing sequence variations

Figure 3 shows the front page of the Mutation@A Glance website. It has two types of query forms, for visualizing known disease mutation data (Fig. 3A) and for evaluating novel genetic variations in query DNA sequences (Fig. 3B). For the visualization, a user inputs a given gene symbol of interest in the form. When the user enters some characters in the form, a list of gene names containing the input character string is shown to assist the user input. In addition, a user can also search for the gene name of interest from an entire list of genes available in Mutation@A Glance, which is displayed by clicking 'Select from List' button (Fig. 3A). Just as information for users, the mutation data set used for each gene is noted near the 'Select from List' button. Figure 4 shows

Mutation@A Glance
Last Update February 17, 2010

Mutation@A Glance

Home Help

Welcome to Mutation@A Glance

This website provides the scientific community with a bioinformatics tool for mutation analysis of causative genes of human diseases. Currently, mutation data of 2656 genes associated with human diseases available in OMIM, UniProt and RAPID (Resource of Asian Primary Immunodeficiency Diseases). To learn how to use this tool, please see [short videos](#) for your guidance. This website works fine on [Firefox](#), [Safari](#) or [Google Chrome](#). If it does not work on your browser, please check [System Requirements](#).

Browse Known Mutations (A)

Please enter a gene symbol of interest, e.g. STAT3, to browse the known mutation data on the nucleotide/amino acid sequences and protein structures.

Gene symbol

Note: Manually curated mutation data is currently available only for [P/Q genes](#) in the RAPID database, and the data for the other genes are retrieved from OMIM and UniProt databases.

Find New Mutations (B)

Please specify a particular gene symbol of interest and paste/upload its DNA sequence data to find and evaluate the mutations occurring in the input sequence(s).

Gene symbol

Paste the DNA sequences (FASTA format)

or

Upload a file for the sequences (FASTA format)

Contact Us / Disclaimer

Figure 3. The front page of Mutation@A Glance. There are two types of query interface for (A) browsing known mutation data and (B) evaluating novel sequence variations in DNA sequences of interest. See the main text for details of the mutation data available in Mutation@A Glance.

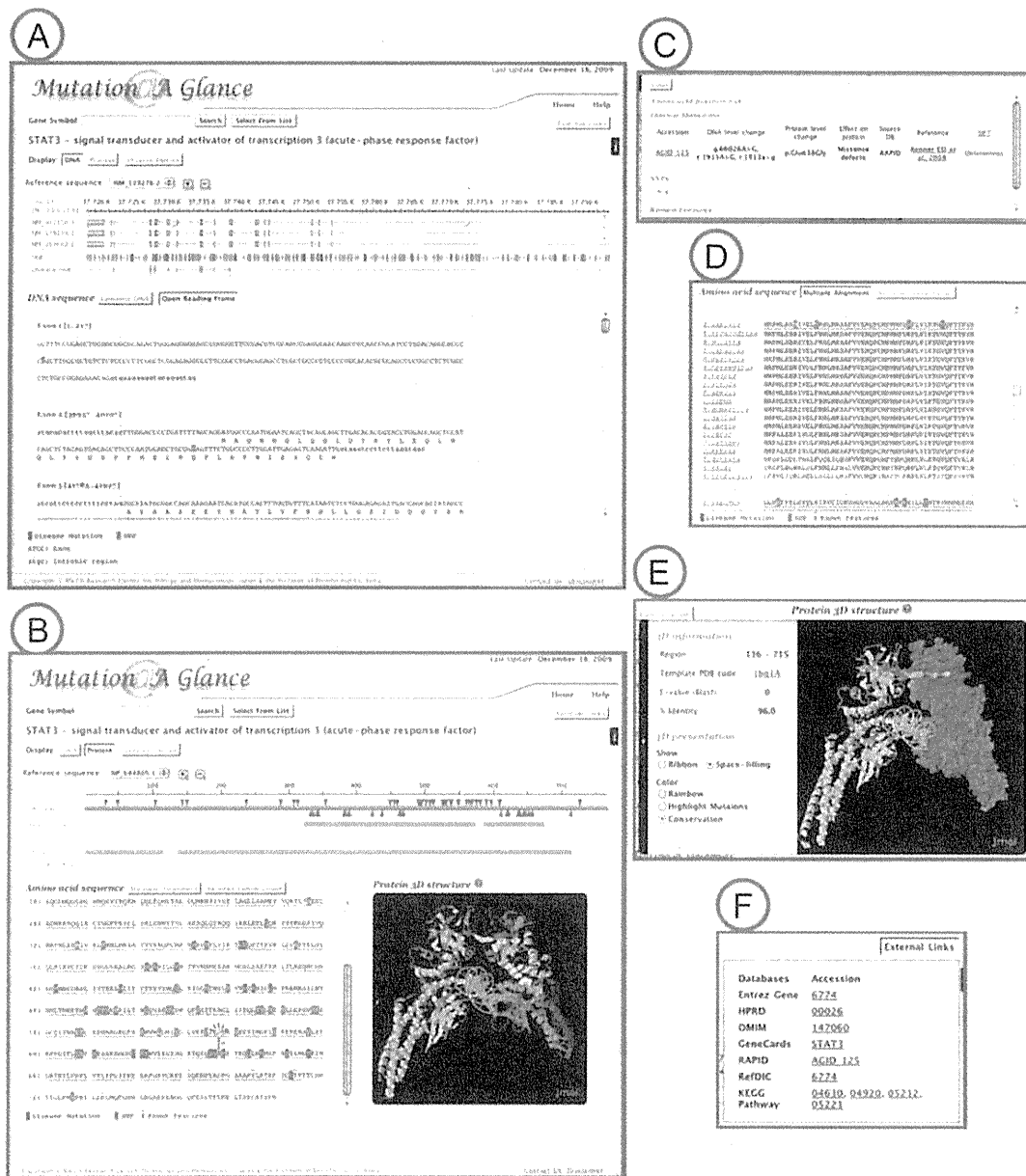


Figure 4. Screenshots of Mutation@A Glance. An example of visualizing mutation data for *STAT3* is shown at the DNA (A) and the protein levels (B). The nucleotide and amino acid positions of disease-associated mutations and SNPs are coloured magenta and green, respectively. At the protein level, various types of information for the mutated amino acid residues can be viewed. (C) The detailed information about the position of nucleotide or amino acid residues selected. (D) A multiple sequence alignment of human and the other organisms *STAT3* protein sequences. (E) Detailed information about the 3D structure displayed with Jmol and the representation option menu for 3D structure information. (F) External links to other website for various types of information about the gene, e.g. gene expression and signalling pathway.

sample screenshots for the *STAT3* gene, which is known to be causative to hyper-IgE syndrome (HIES).^{49,50} At the DNA level, positions of the disease-associated mutations, including substitution, insertion and deletion, as well as SNPs are shown on a set of exon sequences or genomic DNA sequence with/without the open-reading frame for the gene of interest (Fig. 4A). If two or more alternative transcripts exist in the RefSeq database, the genetic variation data are allocated on the reference sequence

that encodes the longest amino acid sequence among the alternative transcripts whereas all the alternative transcripts are indicated in the top panel of the genomic structure. At the protein level, the disease-associated mutation and SNP sites are highlighted in the primary structure of the gene products along with available functional annotation information of the amino acid residues from the UniProt database (e.g. enzymatic active sites and post-translational modification sites, etc.) (Fig. 4B). Information regarding

conserved domain from Pfam (<http://pfam.sanger.ac.uk/>)⁵¹ and predicted intrinsically disordered regions are also displayed. When 3D structure information for the protein is available, the positions of mutation and SNP data can be viewed on the monomer or complex 3D structures with the Jmol applet (Fig. 4B). Detailed information about nucleotide or amino acid residues of interest is displayed in another window after clicking on a residue (Fig. 4C). In particular, at the protein level, an amino acid residue becomes highlighted in the 3D structure when clicking on it (Fig. 4B). The amino acid sequence of human can be compared with those of other organisms by clicking 'Multiple Alignment' button (Fig. 4D). The representation of the 3D structure can be selected from two model types (ribbon or space-filling models) and three colouring types (by rainbow, highlighting mutation positions or residue conservation) (Fig. 4E). The 'External Links' button provides links to NCBI Entrez Gene (<http://www.ncbi.nlm.nih.gov/sites/entrez?db=gene>)⁵² for general information regarding the gene, Human Protein Reference Database (<http://www.hprd.org/>)⁵³ for information about the gene product, GeneCards (<http://www.genecards.org/>)⁵⁴, the Reference Database of Immune Cells (<http://refdic.rcai.riken.jp/>)⁵⁵ for gene expression profiling data and the KEGG pathway (<http://www.genome.jp/>)⁵⁶ for pathways involving this gene (Fig. 4F). By using this visualization facility, mapping amino acid positions of known ns substitutions on the crystal structure of the STAT3–DNA complex (PDB code: 1bg1)⁵⁷ revealed that the disease-associated missense mutation residue positions were spatially located at the interface of the homodimer or at the DNA binding site, whereas the nsSNP residue positions were located on a surface outside of the molecular interaction sites (Fig. 5). This suggests that disease-causative missense mutations in *STAT3* directly affect the protein–protein and/or protein–DNA interaction as reported previously.^{49,50} This is a good demonstration how Mutation@A Glance could help us interpret mutation effects at the molecular level.

3.4. Evaluating the sequence variations in query sequences

One of the issues of diagnosis of genetic diseases is how to evaluate the pathogenicity of newly identified sequence variations. To address this issue, Mutation@A Glance has an interface that allows clinical researchers to assess the impact of an observed sequence variation in a given DNA sequence for a candidate disease-causing gene as the second query form (Fig. 3B). When a user submits DNA sequences of a candidate gene in question, this tool returns a list of sequence variations found in the input DNA sequences at both the DNA and the protein levels

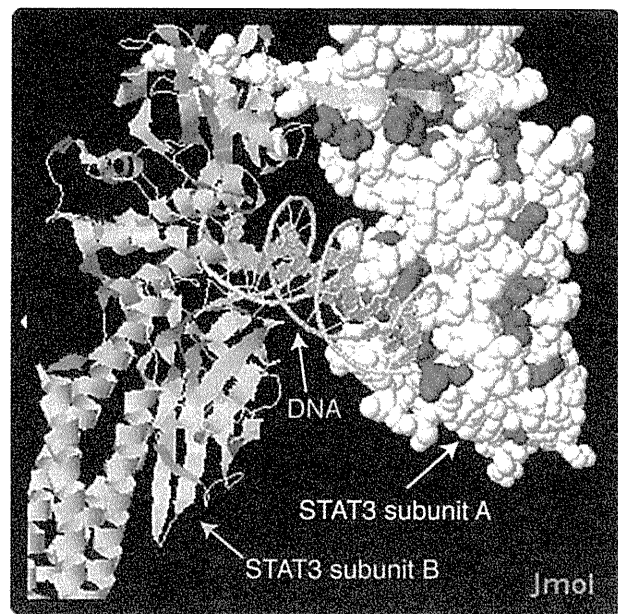


Figure 5. Spatial localization of disease-associated missense mutation sites on the STAT3 protein structure. Two STAT3 subunits are represented as a space-filling model coloured white (subunit A) and a ribbon model coloured pink (subunit B), respectively. A double-stranded DNA is represented as a ribbon model coloured light green. The disease-related missense mutations and nsSNPs of STAT3 (subunit A) are coloured magenta and green, respectively.

(Fig. 6). To identify genetic variations that occur in input DNA sequences of a given gene, the BLAT program⁵⁸ is implemented to align the input DNA sequences with the reference genomic DNA sequence for the corresponding gene. Figure 6A represents the alignment status of the query sequence to the reference sequence. If a sequence variation is found, multiple lines of detailed information about the variation, such as the variation types (e.g. substitution, insertion and deletion), the mutated region (e.g. exon, intron and 5'- or 3'-splice sites constituting the GT-AG rule), the amino acid changes (e.g. missense, nonsense, insertion/deletion and frame-shift), the known variation data (disease-associated mutation and SNP) and structure/function features of the position at the protein level, are displayed based on the reference human genome sequence in the public database (Fig. 6B). Sequence alignments between the query and reference sequences are also displayed (Fig. 6C). If a ns substitution is found in the query DNA sequence, it was evaluated by the SIFT program²⁶ (incorporated in the local system), which predicts whether amino acid substitutions in a protein will be 'Deleterious' or 'Tolerated' using evolutionary information from the homologous proteins (Fig. 6B). We tested the prediction accuracy of SIFT with our data sets of disease-associated mutations and non-disease-associated nsSNPs, and found that the

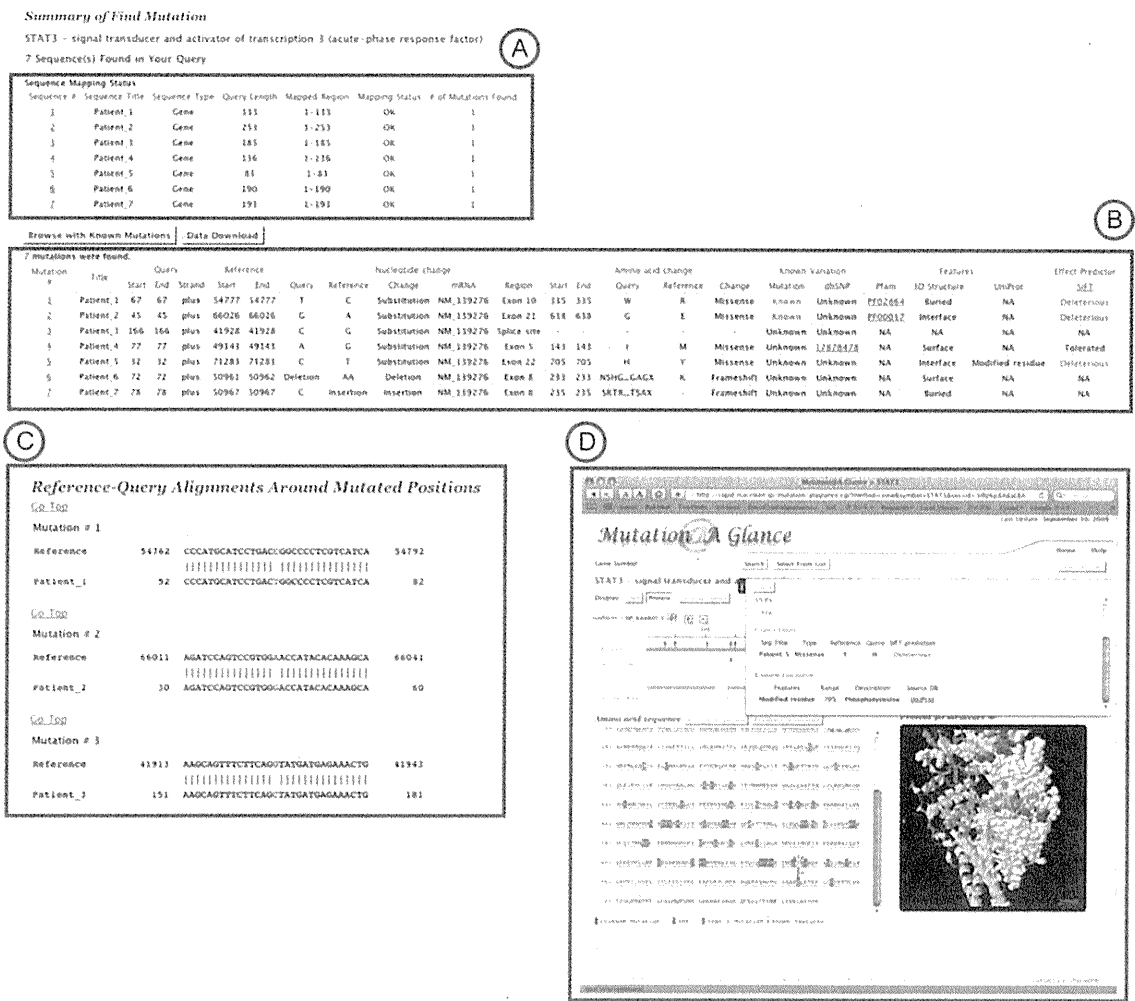


Figure 6. An example of evaluating sequence variations in query *STAT3* DNA sequences. (A) The mapping status of each query sequence to the reference sequence is shown. (B) If a variation is found in the query sequence, the detailed information is shown for each variation (e.g. the positions on the DNA/protein sequences, the type of variation and the description as to whether or not it is known as a disease-associated mutation or SNP). Results from the SIFT program ('Tolerated' or 'Deleterious') are also shown if the variation caused ns substitutions. (C) The query-reference sequence alignment around the altered nucleotides is depicted. (D) The variations can be visualized in the viewer, represented by different colours for known disease mutations or SNPs as 'User's Data'.

false-negative rate (falsely predicted as 'Tolerated' for disease-associated mutations) and the false-positive rate (falsely predicted as 'Deleterious' for nsSNPs) were 25% and 39%, respectively. These accuracy values were comparable to those evaluated in previous study.³³ The current version of Mutation@A Glance does not implement a method for quantitative evaluation of mutation effects on RNA splicing, mainly because we considered the evaluation method is not matured enough yet. However, because the evaluation of mutation effects on RNA splicing/stability is very intriguing, we will place a high priority on the implementation of the evaluation tool for genetic variations affecting RNA splicing/stability in the future development.

There are several advantages of Mutation@A Glance over other existing web servers for evaluating the

effects of mutations. First, users are only required to have DNA sequences from a particular gene as their input and thus do not need to pre-process their submission data; other websites for evaluating the mutation effects require a list of genetic variations as a query, not raw sequence data.²⁶⁻³¹ Secondly, Mutation@A Glance identifies and addresses multiple types of sequence variations (e.g. insertion/deletion, frame-shifts) from input query DNA sequences whereas the other web servers do not. Thirdly, newly identified genetic variations can be easily compared with known mutation and SNP data using the graphical visualization interface of Mutation@A Glance (Fig. 6D).

From a viewpoint of clinical use, it is obvious that any mutation analysis platform cannot serve as a useful one without reliable mutation data sets. However, whereas large amounts of disease-associated mutation

data for various genetic diseases have been reported, most of them are dispersed and stored locally. Only a few websites, e.g. OMIM and UniProt, integrate disease-associated mutation data and allow us to download their contents. However, the mutation data in such databases have a relatively low integrity in terms of updating and coverage. Thus, we have begun to comprehensively collect and manually curate the disease-associated mutation data from published literature focusing on PIDs and established a resource of PID research for clinical use, named RAPID.¹⁷ Mutation@A Glance thus uses these manually curated data sets for over 150 PID genes in the RAPID database, which is solid enough for clinical use at least for PID analysis. To make Mutation@A Glance a reliable and general mutation analysis platform for other various genetic diseases in the future, we consider that data sharing with experts in particular diseases will be highly important as in the case of PID; otherwise it would take a long time to accumulate extensive mutation data of all human disease genes to an acceptable level for clinical use. In fact, similar efforts along this direction have been being made by the research community.¹⁹

As new technologies for determining genetic variation in humans have rapidly and continuously emerged (such as next generation DNA sequencing), amounts of genetic variation data of human are exponentially growing.^{6,7,59} Therefore, we will continue to update and improve the Mutation@A Glance system, in order to cope with the larger-scale data analysis for more comprehensive identification of disease-causative candidate genes. Implementing API programs into Mutation@A Glance for query submissions and a retrieval system through command line scripts would be more convenient for this purpose.

In summary, Mutation@A Glance provides a highly integrated bioinformatics tool for mutation analysis not only for facilitating visualization of sequence variation data along with various types of information, including primary and tertiary structures of the gene products, but also for evaluating the effects of novel sequence variations in a query input DNA sequence. This tool works solely on a web browser through Internet and is open to the public. Hence, Mutation@A Glance can be used as a 'one-stop' integrated bioinformatics platform for analysing genotype–phenotype relationships of genetic diseases from molecular as well as clinical perspectives.

Acknowledgements: The authors would like to thank Drs Shigeaki Nonoyama, Kohsuke Imai, Hirokazu Kanegane, Toshio Miyawaki, Koichi Oshima, Fumihiko Ishikawa and Reiko Kikuno-Fukaya for their critical suggestions about this work.

Supplementary Data: Supplementary Data are available at www.dnaresearch.oxfordjournals.org.

Funding

This work is supported by a Grant-in-aid for Special Coordination Funds for Promoting Science and Technology, from the Ministry of Education, Culture, Sports, Science and Technology of Japan.

References

1. Amberger, J., Bocchini, C.A., Scott, A.F. and Hamosh, A. 2009, McKusick's Online Mendelian Inheritance in Man (OMIM), *Nucleic Acids Res.*, **37**, D793–6.
2. Notarangelo, L., Casanova, J.L., Fischer, A., et al. 2004, Primary immunodeficiency diseases: an update, *J. Allergy Clin. Immunol.*, **114**, 677–87.
3. Geha, R.S., Notarangelo, L.D., Casanova, J.L., et al. 2007, Primary immunodeficiency diseases: an update from the International Union of Immunological Societies Primary Immunodeficiency Diseases Classification Committee, *J. Allergy Clin. Immunol.*, **120**, 776–94.
4. Notarangelo, L.D. and Sorensen, R. 2008, Is it necessary to identify molecular defects in primary immunodeficiency disease?, *J. Allergy Clin. Immunol.*, **122**, 1069–73.
5. Frazer, K.A., Ballinger, D.G., Cox, D.R., et al. 2007, A second generation human haplotype map of over 3.1 million SNPs, *Nature*, **449**, 851–61.
6. Kryukov, G.V., Shpunt, A., Stamatoyannopoulos, J.A. and Sunyaev, S.R. 2009, Power of deep, all-exon resequencing for discovery of human trait genes, *Proc. Natl Acad. Sci. USA*, **106**, 3871–6.
7. Chun, S. and Fay, J.C. 2009, Identification of deleterious mutations within three human genomes, *Genome Res.*, **19**, 1553–61.
8. Sunyaev, S., Ramensky, V., Koch, I., Lathe, W. III, Kondrashov, A.S. and Bork, P. 2001, Prediction of deleterious human alleles, *Hum. Mol. Genet.*, **10**, 591–7.
9. Tavtigian, S.V., Byrnes, G.B., Goldgar, D.E. and Thomas, A. 2008, Classification of rare missense substitutions, using risk surfaces, with genetic- and molecular-epidemiology applications, *Hum. Mutat.*, **29**, 1342–54.
10. Tavtigian, S.V., Greenblatt, M.S., Goldgar, D.E. and Boffetta, P. 2008, Assessing pathogenicity: overview of results from the IARC Unclassified Genetic Variants Working Group, *Hum. Mutat.*, **29**, 1261–4.
11. Tavtigian, S.V., Greenblatt, M.S., Lesueur, F. and Byrnes, G.B. 2008, In silico analysis of missense substitutions using sequence-alignment based methods, *Hum. Mutat.*, **29**, 1327–36.
12. Houdayer, C., Dehainault, C., Mattler, C., et al. 2008, Evaluation of in silico splice tools for decision-making in molecular diagnosis, *Hum. Mutat.*, **29**, 975–82.
13. Stenson, P.D., Mort, M., Ball, E.V., et al. 2009, The Human Gene Mutation Database: 2008 update, *Genome Med.*, **1**, 13.

14. Singh, A., Olowoyeye, A., Baenziger, P.H., et al. 2008, MutDB: update on development of tools for the biochemical analysis of genetic variation, *Nucleic Acids Res.*, **36**, D815–9.
15. Mailman, M.D., Feolo, M., Jin, Y., et al. 2007, The NCBI dbGaP database of genotypes and phenotypes, *Nat. Genet.*, **39**, 1181–6.
16. Piirila, H., Valiaho, J. and Vihinen, M. 2006, Immunodeficiency mutation databases (IDbases), *Hum. Mutat.*, **27**, 1200–8.
17. Keerthikumar, S., Raju, R., Kandasamy, K., et al. 2009, RAPID: Resource of Asian Primary Immunodeficiency Diseases, *Nucleic Acids Res.*, **37**, D863–7.
18. Sherry, S.T., Ward, M.H., Kholodov, M., et al. 2001, dbSNP: the NCBI database of genetic variation, *Nucleic Acids Res.*, **29**, 308–11.
19. Kaput, J., Cotton, R.G., Hardman, L., et al. 2009, Planning the human variome project: the Spain report, *Hum. Mutat.*, **30**, 496–510.
20. Lee, P.H. and Shatkay, H. 2008, F-SNP: computationally predicted functional SNPs for disease association studies, *Nucleic Acids Res.*, **36**, D820–4.
21. Yuan, H.Y., Chiou, J.J., Tseng, W.H., et al. 2006, FASTSNP: an always up-to-date and extendable service for SNP function analysis and prioritization, *Nucleic Acids Res.*, **34**, W635–41.
22. Yue, P., Melamud, E. and Moul, J. 2006, SNPs3D: candidate gene and SNP selection for association studies, *BMC Bioinformatics*, **7**, 166.
23. Chelala, C., Khan, A. and Lemoine, N.R. 2009, SNPnexus: a web database for functional annotation of newly discovered and public domain single nucleotide polymorphisms, *Bioinformatics*, **25**, 655–61.
24. Yang, J.O., Hwang, S., Oh, J., Bhak, J. and Sohn, T.K. 2008, An integrated database-pipeline system for studying single nucleotide polymorphisms and diseases, *BMC Bioinformatics*, **9** (Suppl 12), S19.
25. Frezal, J. 1998, Genatlas database, genes and development defects, *C. R. Acad. Sci. III*, **321**, 805–17.
26. Ng, P.C. and Henikoff, S. 2003, SIFT: predicting amino acid changes that affect protein function, *Nucleic Acids Res.*, **31**, 3812–4.
27. Ramensky, V., Bork, P. and Sunyaev, S. 2002, Human non-synonymous SNPs: server and survey, *Nucleic Acids Res.*, **30**, 3894–900.
28. Thomas, P.D., Campbell, M.J., Kejariwal, A., et al. 2003, PANTHER: a library of protein families and subfamilies indexed by function, *Genome Res.*, **13**, 2129–41.
29. Bromberg, Y. and Rost, B. 2007, SNAP: predict effect of non-synonymous polymorphisms on function, *Nucleic Acids Res.*, **35**, 3823–35.
30. Ferrer-Costa, C., Gelpi, J.L., Zamakola, L., Parraga, I., de la Cruz, X. and Orozco, M. 2005, PMUT: a web-based tool for the annotation of pathological mutations on proteins, *Bioinformatics*, **21**, 3176–8.
31. Bao, L., Zhou, M. and Cui, Y. 2005, nsSNPAnalyzer: identifying disease-associated nonsynonymous single nucleotide polymorphisms, *Nucleic Acids Res.*, **33**, W480–2.
32. Thusberg, J. and Vihinen, M. 2009, Pathogenic or not? And if so, then how? Studying the effects of missense mutations using bioinformatics methods, *Hum. Mutat.*, **30**, 703–14.
33. Ng, P.C. and Henikoff, S. 2006, Predicting the effects of amino acid substitutions on protein function, *Annu. Rev. Genomics Hum. Genet.*, **7**, 61–80.
34. Boutet, E., Lieberherr, D., Tognolli, M., Schneider, M. and Bairoch, A. 2007, UniProtKB/Swiss-Prot, *Methods Mol. Biol.*, **406**, 89–112.
35. Altschul, S.F., Gish, W., Miller, W., Myers, E.W. and Lipman, D.J. 1990, Basic local alignment search tool, *J. Mol. Biol.*, **215**, 403–10.
36. Thompson, J.D., Higgins, D.G. and Gibson, T.J. 1994, CLUSTAL W: improving the sensitivity of progressive multiple sequence alignment through sequence weighting, position-specific gap penalties and weight matrix choice, *Nucleic Acids Res.*, **22**, 4673–80.
37. Berman, H.M., Battistuz, T., Bhat, T.N., et al. 2002, The Protein Data Bank, *Acta Crystallogr. D Biol. Crystallogr.*, **58**, 899–907.
38. Marti-Renom, M.A., Stuart, A.C., Fiser, A., Sanchez, R., Melo, F. and Sali, A. 2000, Comparative protein structure modeling of genes and genomes, *Annu. Rev. Biophys. Biomol. Struct.*, **29**, 291–325.
39. Shen, M.Y. and Sali, A. 2006, Statistical potential for assessment and prediction of protein structures, *Protein Sci.*, **15**, 2507–24.
40. Shrake, A. and Rupley, J.A. 1973, Environment and exposure to solvent of protein atoms. Lysozyme and insulin, *J. Mol. Biol.*, **79**, 351–71.
41. Ward, J.J., McGuffin, L.J., Bryson, K., Buxton, B.F. and Jones, D.T. 2004, The DISOPRED server for the prediction of protein disorder, *Bioinformatics*, **20**, 2138–9.
42. Sunyaev, S., Ramensky, V. and Bork, P. 2000, Towards a structural basis of human non-synonymous single nucleotide polymorphisms, *Trends Genet.*, **16**, 198–200.
43. Vitkup, D., Sander, C. and Church, G.M. 2003, The amino-acid mutational spectrum of human genetic disease, *Genome Biol.*, **4**, R72.
44. Wang, Z. and Moul, J. 2001, SNPs, protein structure, and disease, *Hum. Mutat.*, **17**, 263–70.
45. Ferrer-Costa, C., Orozco, M. and de la Cruz, X. 2002, Characterization of disease-associated single amino acid polymorphisms in terms of sequence and structure properties, *J. Mol. Biol.*, **315**, 771–86.
46. Kono, H., Yuasa, T., Nishiue, S. and Yura, K. 2008, coliSNP database server mapping nsSNPs on protein structures, *Nucleic Acids Res.*, **36**, D409–13.
47. Chen, J.W., Romero, P., Uversky, V.N. and Dunker, A.K. 2006, Conservation of intrinsic disorder in protein domains and families: I. A database of conserved predicted disordered regions, *J. Proteome Res.*, **5**, 879–87.
48. Schuster-Bockler, B. and Bateman, A. 2008, Protein interactions in human genetic diseases, *Genome Biol.*, **9**, R9.
49. Holland, S.M., DeLeo, F.R., Elloumi, H.Z., et al. 2007, STAT3 mutations in the hyper-IgE syndrome, *N. Engl. J. Med.*, **357**, 1608–19.
50. Minegishi, Y., Saito, M., Tsuchiya, S., et al. 2007, Dominant-negative mutations in the DNA-binding

- domain of STAT3 cause hyper-IgE syndrome, *Nature*, **448**, 1058–62.
51. Finn, R.D., Tate, J., Mistry, J., et al. 2008, The Pfam protein families database, *Nucleic Acids Res.*, **36**, D281–8.
52. Sayers, E.W., Barrett, T., Benson, D.A., et al. 2009, Database resources of the National Center for Biotechnology Information, *Nucleic Acids Res.*, **37**, D5–15.
53. Keshava Prasad, T.S., Goel, R., Kandasamy, K., et al. 2009, Human Protein Reference Database—2009 update, *Nucleic Acids Res.*, **37**, D767–72.
54. Rebhan, M., Chalifa-Caspi, V., Prilusky, J. and Lancet, D. 1998, GeneCards: a novel functional genomics compendium with automated data mining and query reformulation support, *Bioinformatics*, **14**, 656–64.
55. Hijikata, A., Kitamura, H., Kimura, Y., et al. 2007, Construction of an open-access database that integrates cross-reference information from the transcriptome and proteome of immune cells, *Bioinformatics*, **23**, 2934–41.
56. Kanehisa, M. and Goto, S. 2000, KEGG: kyoto encyclopedia of genes and genomes, *Nucleic Acids Res.*, **28**, 27–30.
57. Becker, S., Groner, B. and Muller, C.W. 1998, Three-dimensional structure of the Stat3beta homodimer bound to DNA, *Nature*, **394**, 145–51.
58. Kent, W.J. 2002, BLAT—the BLAST-like alignment tool, *Genome Res.*, **12**, 656–64.
59. Ahn, S.M., Kim, T.H., Lee, S., et al. 2009, The first Korean genome sequence and analysis: full genome sequencing for a socio-ethnic group, *Genome Res.*, **19**, 1622–9.

1. 先天性免疫不全症における 低ガンマグロブリン血症

金兼 弘和*・宮脇 利男**
Kanegane Hirokazu Miyawaki Toshio

*富山大学附属病院 小児科 講師

**富山大学大学院 医学薬学研究部 小児科 教授

Summary

先天性免疫不全症とは、生体防御機構（免疫系）の破綻により易感染性を呈する比較的稀な疾患である。先天性免疫不全症のうち抗体産生不全症、すなわち低ガンマグロブリン血症を呈する疾患の治療は免疫グロブリン補充療法であり、半世紀以上の歴史がある。さらに、この20年間に多くの先天性免疫不全症の分子病態が明らかになりつつあるが、いまだに多くの患者が未診断あるいは診断の遅れのため後遺症に悩み、生活の質を落としている。本稿では免疫グロブリン補充療法の適応となる低ガンマグロブリン血症の診断と治療の最前線について概説する。

はじめに

低ガンマグロブリン血症は、一般的には血清免疫グロブリン値が正常値の-2SD以下に低下したものと定義づけられ、先天性のものと感染症、悪性腫瘍、免疫抑制剤や抗てんかん薬を含む薬剤投与などによる続発性のものがある。続発性のものについては本特集にて他の著者らが解説しており、本稿では先天性免疫不全症における低ガンマグロブリン血症のみについて解説する。低ガンマグロブリン血症は臨床的には肺炎や中耳炎などの細菌感染症を繰り返すことで気づかれ、治療の基本は免疫グロブリン補充療法と抗菌薬投与である。代表的疾患はX連鎖無ガンマグロブリン血症(X-linked agammaglobulinemia : XLA)であり、

その原因遺伝子はプロB細胞からプレB細胞の分化に必要な *Bruton's tyrosine kinase (BTK)* である^{1, 2)}。BTK以外にも、B細胞分化障害を来し得るすべての遺伝子異常が低ガンマグロブリン血症となる。B細胞分化段階のどのレベルでの障害かによっていくつかに分類することが可能であり、そのように考えると低ガンマグロブリン血症を理解しやすい。

1. B細胞分化

B細胞は骨髄において造血幹細胞 (hematopoietic stem cells : HSC) から抗原非依存性にプロB細胞、プレB細胞、未熟B細胞と分化し、末梢血に流出する。末梢血においては抗原依存性に

XLA (X-linked agammaglobulinemia ; X連鎖無ガンマグロブリン血症) BTK (*Bruton's tyrosine kinase*)
HSC (hematopoietic stem cells ; 造血幹細胞)

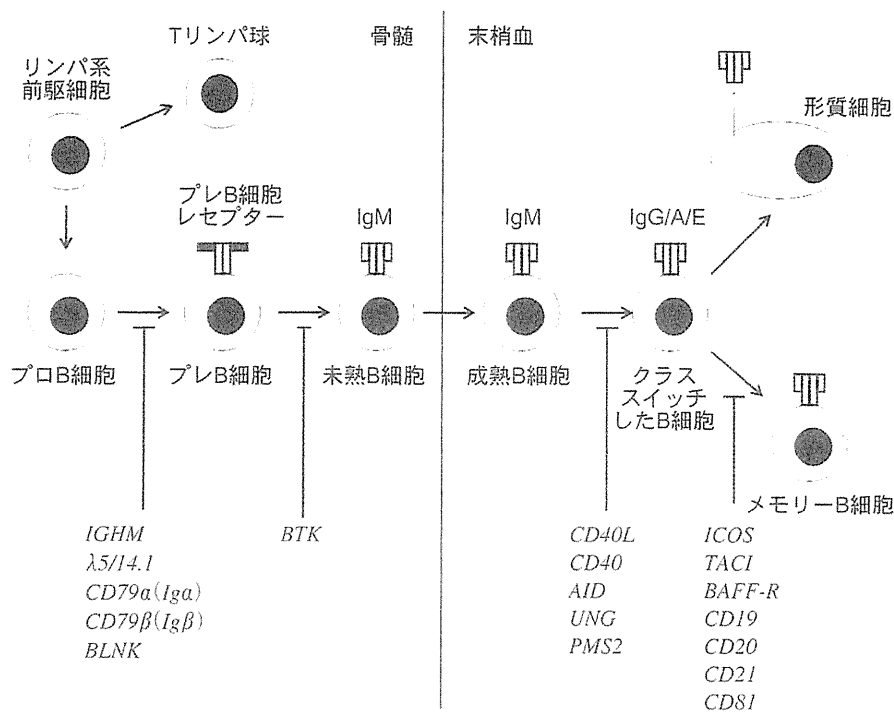


図1 B細胞分化と低ガンマグロブリン血症

リンパ系前駆細胞からプロB細胞、プレB細胞、未熟B細胞を経て成熟B細胞となり、最終的には形質細胞へと分化して免疫グロブリン産生を行う。この分化過程に異常が認められると、低ガンマグロブリン血症となる。

(Wood P : Ann Clin Biochem 2009 より一部改変)

ナイーブB細胞からメモリーB細胞へと分化し、最終的には形質細胞となり、免疫グロブリン産生を行う。この分化段階のいずれかに異常があっても、最終的には低ガンマグロブリン血症となり得る(図1)。

低ガンマグロブリン血症の代表的疾患であるXLAは、*BTK*変異によって発症する。*BTK*はプレB細胞レセプターからのシグナル伝達に重要な働きをしており、*BTK*欠損によりプロB細胞からプレB細胞への分化障害が生じる。プレB細胞レセプターはμ重鎖、λ5、VpreB、Igα、Igβから構成され、VpreBを除くすべての遺伝子変異による常染色体劣性無ガンマグロブリン血症が報告され

ている^{3~9)}。さらに、プレB細胞からのシグナルを下流に伝えるアダプター分子としてBLNKが存在し、*BLNK*変異によっても無ガンマグロブリン血症を生じる¹⁰⁾。

末梢血にB細胞は存在するが、低ガンマグロブリン血症を呈する疾患群として分類不能型免疫不全症(common variable immunodeficiency: CVID)がある。その基本病態はナイーブB細胞からメモリーB細胞への分化障害である。CVIDについての詳細は別稿に譲る。

また、末梢血B細胞はIgMおよびIgDのみを産生するB細胞からすべてのクラスの免疫グロブリンを産生するB細胞へ分化するが、この分化段階

CVID (common variable immunodeficiency ; 分類不能型免疫不全症)

表1 抗体産生不全症

疾患	遺伝子異常 / 産物
B細胞の著明な減少を伴いすべてのクラスの免疫グロブリン低下を伴うもの	
BTK 欠損症 (XLA)	<i>BTK/BTK</i>
μ 重鎖欠損症	<i>IGHM/μ</i> 重鎖
λ 5 欠損症	<i>CD179B/λ</i> 5
Ig α 欠損症	<i>CD79A/Ig α</i>
Ig β 欠損症	<i>CD79B/Ig β</i>
BLNK 欠損症	<i>BLNK/BLNK</i>
免疫不全を伴う胸腺腫 (Good 症候群)	不明
骨髄異形成症候群	モノソミー 7, トリソミー 8
先天性角化不全症	<i>DKC1/Dyskerin</i>
B細胞数は正常から低値をとり IgG および IgA の著明な減少と伴うもの	
分類不能型免疫不全症 (CVID)	<i>TNFRSF13B/TACI</i> <i>TNFRSF13C/BAFF-R</i>
ICOS 欠損症	<i>ICOS/ICOS</i>
CD19 欠損症	<i>CD19/CD19</i>
CD81 欠損症	<i>CD81/CD81</i>
CD20 欠損症	<i>CD20/CD20</i>
CD21 欠損症	<i>CD21/CD21</i>
X連鎖リンパ増殖症候群 (XLP)	<i>SH2D1A/SAP</i> <i>BIRC4/XIAP</i>
B細胞数は正常であり IgG および IgA は減少するが IgM は正常または高値であるもの	
CD40L 欠損症 (X連鎖高 IgM 症候群)	<i>TNFSF5/CD154 (CD40L)</i>
CD40 欠損症	<i>TNFSF5/CD40</i>
AID 欠損症	<i>AICDA/AID</i>
UNG 欠損症	<i>UNG/UNG</i>
PMS2 欠損症	<i>PMS2/PMS2</i>

(文献 17 より一部改変)

に異常があった場合には、いわゆる高 IgM 症候群 (hyper-IgM syndrome : HIGM) となる。その原因遺伝子として *CD154 (CD40L)* のみならず^{11, 12)}, *CD40*, *Activation-induced cytidine deaminase (AID)*, *Uracil-DNA glycosylase (UNG)*, *PMS2* が報告されている^{13~16)}。

低ガンマグロブリン血症の分類と原因遺伝子について表 1 に示す¹⁷⁾。

2. 低ガンマグロブリン血症を呈する先天性免疫不全症

1) B細胞の著明な減少を伴いすべてのクラスの免疫グロブリン低下を伴うもの

① X連鎖無ガンマグロブリン血症

このカテゴリーに属する代表的疾患は XLA である。XLA は 1952 年にアメリカの小児科医 Bruton¹⁸⁾ によって最初に報告され、先天性免疫

HIGM (hyper-IgM syndrome ; 高 IgM 症候群) *AID* (*Activation-induced cytidine deaminase*)
UNG (*Uracil-DNA glycosylase*)

不全症の診断と治療の歴史は、この報告から始まるといっても過言ではない。疾患の同定から約40年後の1993年にXLAの原因遺伝子が2つのグループから報告され^{1, 2)}、*BTK*と命名された。*BTK*はXq22に局在し、19のエクソンからなる37 kbの遺伝子であり、細胞内チロシンキナーゼであるTECファミリーに属し、形質細胞を除くすべてのB細胞、骨髄細胞、単球、血小板に発現しているが、T細胞には発現していない。*BTK*はリン酸化蛋白であり、プレB細胞からのシグナル伝達に重要な働きをし、*BTK*変異によってプロB細胞からプレB細胞への分化障害が生じ、その結果としてB細胞欠損による無ガンマグロブリン血症となる。

臨床症状は母親からの移行抗体の消失する生後4カ月過ぎから肺炎や中耳炎などの細菌感染を繰り返すようになって気づかれ、多くは5歳までに診断されるが、大人になって初めて診断される例も稀ではない。また、通常ウイルス感染に対しては抵抗性であるが、エンテロウイルスに対しては易感染性を示す。家族歴があれば診断は容易であるが、家族歴を有するものは半数以下である。よって、家族歴がなくても易感染性を示す男児で、血清免疫グロブリン低値で、末梢血B細胞欠損を伴う場合には積極的にXLAを疑う。

② 常染色体劣性無ガンマグロブリン血症

B細胞欠損を伴う先天性無ガンマグロブリン血症の約15%では*BTK*遺伝子変異が同定されず、常染色体劣性無ガンマグロブリン血症と称される。そのうち20～30%は μ 重鎖欠損症である^{3, 4)}。それ以外にもごく数家系ずつであるが、 $\lambda 5$ 、*Ig α* 、*Ig β* 、*BLNK*変異による無ガンマグロブリン血症が報告されている^{5~10)}。臨床的にはXLAとほとんど同じであるが、発症年齢が早く、エンテロウイルス感染を含む重症感染症に罹患し

やすいとされている。恐らくVpreBを始めとするプレB細胞レセプター・コンプレックスならびにそのシグナル伝達分子による無ガンマグロブリン血症が存在すると思われる。

2) B細胞数は正常から低値をとりIgGおよびIgAの著明な減少を伴うもの

① 分類不能型免疫不全症

XLAと並んで低ガンマグロブリン血症の代表的疾患であるが、詳細は別稿に譲る。

② X連鎖リンパ増殖症候群

XLPはEBウイルス(EBV)感染に対する特異的免疫応答の欠陥を有する先天性免疫不全症であり、臨床的表現として致死的伝染性単核症(60%)、悪性リンパ腫(30%)のほかに、低ガンマグロブリン血症(30%)もある。多くはEBV感染症後であるが、一部にはEBV感染症の既往が明らかでない場合もある。原因遺伝子は*SH2D1A*(タイプ1)だけでなく、*BIRC4*(タイプ2)の2種類がある^{19~21)}。

3) B細胞数は正常でありIgGおよびIgAは減少するがIgMは正常または高値であるもの

① X連鎖高IgM症候群

IgGおよびIgAは正常であるが、IgMが正常または高値であるということはクラススイッチの異常を示唆し、X連鎖HIGMの原因遺伝子はT細胞上に存在する*CD154*(CD40リガンド)と同定された^{11, 12)}。CD154はB細胞上のCD40との相互作用でクラススイッチに関わっている。X連鎖HIGMはニューモシスチス肺炎を始めとする細胞性免疫異常としての症状を呈し、臨床的には複合免疫不全症と捉えられ、造血幹細胞移植の適応でもある。

② 常染色体劣性高IgM症候群

HIGMにおける高IgM血症は繰り返す感染症

EBV (EBウイルス)

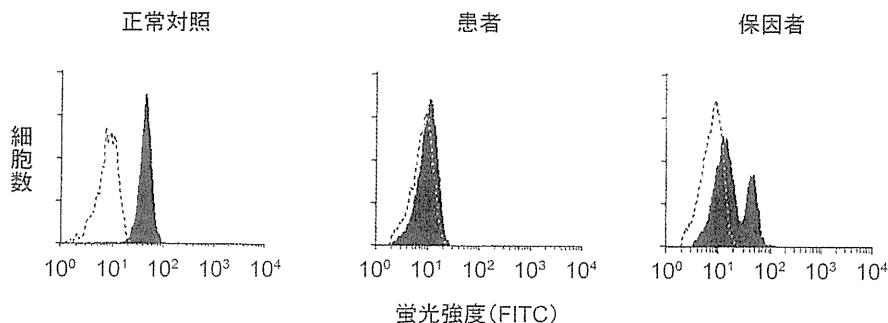


図2 フローサイトメトリーによる単球内 BTK 蛋白の発現

抗BTKモノクローナル抗体による染色は黒塗り、コントロール抗体による染色は点線で示す。正常対照ではBTK蛋白の発現を認めるが、XLA患者ではBTK蛋白の発現が低下し、保因者ではモザイクパターンをとる。(筆者作成)

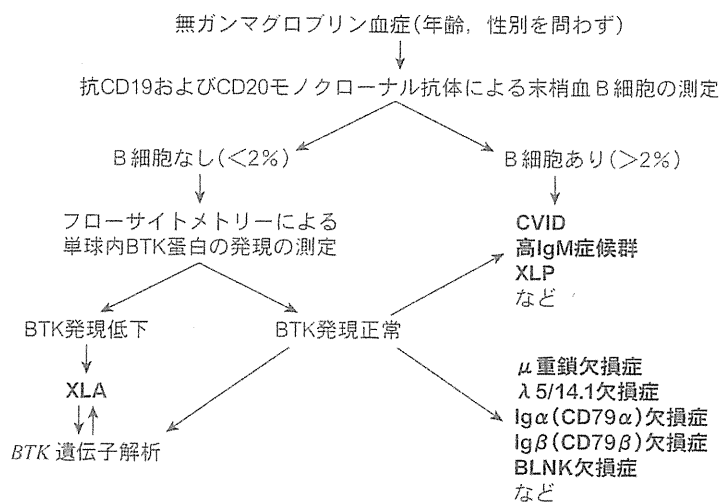


図3 低ガンマグロブリン血症の診断フローチャート

低ガンマグロブリン血症の患者をみた場合には、このフローチャートに従って診断を進める。太字は疾患名を示す。(筆者作成)

の結果としての検査値であり、病気の本態から考えて「クラススイッチ異常症」と呼ぶ方がふさわしい。HIGMの原因遺伝子としてクラススイッチに関わる分子が精力的に調べられ、CD40, AID, UNG, PMS2が同定されている¹³⁻¹⁶⁾。

3. 診断

繰り返す細菌感染症より低ガンマグロブリン血症が疑われる場合には、まずは血清免疫グロブリン値 (IgG, IgA, IgM) を測定し、さらにリンパ球サブセットにてB細胞の有無をチェックする。

XLAの診断は最終的には *BTK* 遺伝子変異を確認する必要があるが³, フローサイトメトリーにて単球内の *BTK* 蛋白の発現を調べることによって迅速診断可能であり, 本方法では保因者診断も可能である(図2)^{22, 23)}. XLPもフローサイトメトリーによるスクリーニングが可能である²⁴⁾. 最終診断は遺伝子解析によるが³, 原因不明のものも多く, やみくもに遺伝子解析を行うのも労力の無駄である。まずはフローサイトメトリーにてスクリーニングを行った後に, 遺伝子解析へと進める(図3)。

患者のフォローにあたっては, 副鼻腔炎や気管支拡張症などの慢性呼吸器感染症の合併に留意する(図4)。潜在性に慢性化している場合が少なからずあるので, 定期的な呼吸機能検査, レ線, 胸部CT, 喀痰培養を怠らない。

4. 治療

治療は, 急性期における適切な抗菌薬投与と, 免疫グロブリン定期補充療法である。IgG トラフ値を少なくとも 500 mg/dL 以上に保つように, 3~4週間毎に 200~600 mg/kg の免疫グロブリンを補充する。これまでは保険適応の制限があり, 十分な投与が行われていない患者も少なからず存在していたが, 今回の改訂によりすべての患者がようやく諸外国と同レベルの治療を受けることができるようになった。気管支拡張症などの慢性呼吸器感染症を合併している場合には, IgG トラフ値は 800 mg/dL 以上に保つようにしたい。海外では在宅での皮下注療法や高濃度(10%)製剤による補充療法が行われており, 患者 QOL の向上に繋がっている。早くわが国においても実現できるよう望みたい。原因遺伝子がわかっているものでは理論的には遺伝子治療が可能であり, 現在基礎的研究も勢力的に行われており, その臨床的応用に今後期待したい。

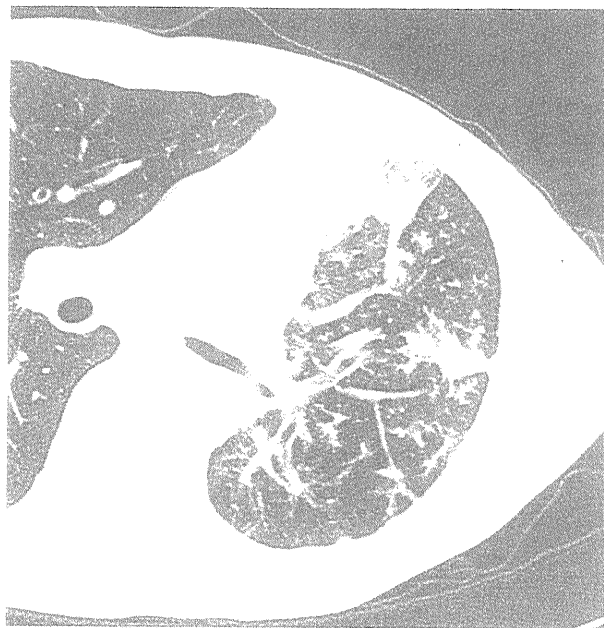


図4 XLA患者の胸部CT所見

22歳のXLA患者における胸部CT所見を示す。左肺野に肺炎ならびに気管支拡張症を認める。(筆者提供)

おわりに

低ガンマグロブリン血症は決してXLAやCVIDだけではなく, さまざまな原因遺伝子が同定されている。その病態はB細胞分化障害と捉えると理解しやすい。もし診断や治療に困る症例があれば, 筆者らまで連絡していただければ幸いです。

文献

- 1) Vetrie D, Vorechovský I, Sidera P, et al: The gene involved in X-linked agammaglobulinemia is a member of the src family of protein-tyrosine kinases. *Nature* 361: 226-233, 1993
- 2) Tsukada S, Saffran DC, Rawlings DJ, et al: Deficient expression of a B cell cytoplasmic tyrosine kinase in human X-linked agammaglobulinemia. *Cell* 72: 279-290, 1993
- 3) Yel L, Minegishi Y, Coustan E, et al: Mutations in the μ heavy-chain gene in patients with

- agammaglobulinemia. *N Engl J Med* **335** : 1486-1493, 1996
- 4) Lopez GE, Porgiglia AS, Hogan MB, et al : Clinical and molecular analysis of patients with defects in micro heavy chain gene. *J Clin Invest* **110** : 1029-1035, 2002
 - 5) Minegishi Y, Coustan-Smith E, Wang YH, et al : Mutations in the human 5/14.1 gene result in B cell deficiency and agammaglobulinemia. *J Exp Med* **187** : 71-77, 1998
 - 6) Minegishi Y, Coustan-Smith E, Rapalus L, et al : Mutations in Ig (CD79a) result in a complete block in B-cell development. *J Clin Invest* **104** : 1115-1121, 1999
 - 7) Wang Y, Kanegane H, Sanal O, et al : Novel Ig (CD79a) gene mutation in a Turkish patient with B cell deficiency and agammaglobulinemia. *Am J Med Genet* **108** : 333-336, 2002
 - 8) Ferrari S, Lougaris V, Caraffi S, et al : Mutations of the Ig β gene cause agammaglobulinemia in man. *J Exp Med* **204** : 2047-2051, 2007
 - 9) Dobbs AK, Yang T, Farmer D, et al : A hypomorphic mutation in Ig β (CD79b) in a patient with immunodeficiency and a leaky defect in B cell development. *J Immunol* **179** : 2055-2059, 2007
 - 10) Minegishi Y, Rohrer J, Coustan-Smith E, et al : An essential role for BLNK in human B cell development. *Science* **286** : 1954-1957, 1999
 - 11) Aruffo A, Farrington M, Hollenbaugh D, et al : The CD40 ligand, gp39, is defective in activated T cells from patients with X-linked hyper-IgM syndrome. *Cell* **72** : 291-300, 1993
 - 12) DiSanto JP, Bonnefoy JY, Gauchatt JF, et al : CD40 ligand mutations in X-linked immunodeficiency with hyper-IgM. *Nature* **361** : 541-543, 1993
 - 13) Ferrari S, Giliani S, Insalaco A, et al : Mutations of CD40 gene cause an autosomal recessive form of immunodeficiency with hyper IgM. *Proc Natl Acad Sci USA* **98** : 12614-12619, 2001
 - 14) Revy P, Muto T, Levy Y, et al : Activation-induced cytidine deaminase (AID) deficiency causes the autosomal recessive form of the hyper-IgM syndrome (HIGM2). *Cell* **102** : 565-575, 2000
 - 15) Imai K, Slupphaug G, Lee WI, et al : Human uracil-DNA glycosylase deficiency associated with profoundly impaired immunoglobulin class-switch recombination. *Nat Immunol* **112** : 755-760, 2003
 - 16) Peron S, Metin A, Gardes P, et al : Human PMS2 deficiency is associated with impaired immunoglobulin class switch recombination. *J Exp Med* **205** : 2465-2472, 2008
 - 17) Yong PFK, Chee R, Grimbacher B : Hypogammaglobulinemia. *Immunol Allergy Clin N Am* **28** : 691-713, 2008
 - 18) Bruton OC : Agammaglobulinemia. *Pediatrics* **9** : 722-728, 1952
 - 19) Coffey AJ, Brooksbank RA, Brandau O, et al : Host response to EBV infection in X-linked lymphoproliferative diseases results from mutations in an SH2-domain encoding gene. *Nat Genet* **20** : 129-135, 1998
 - 20) Sayos J, Wu C, Morra M, et al : The X-linked lymphoproliferative-disease gene product SAP regulates signals induced through the coreceptor SLAM. *Nature* **395** : 462-469, 1998
 - 21) Rigaud S, Fondanèche MC, Lambert N, et al : XIAP deficiency in humans causes an X-linked lymphoproliferative syndrome. *Nature* **444** : 110-114, 2006
 - 22) Futatani T, Miyawaki T, Tsukada S, et al : Deficient expression of Bruton's tyrosine kinase in monocytes from X-linked agammaglobulinemia as evaluated by a flow cytometric analysis and its clinical application to carrier detection. *Blood* **91** : 595-602, 1998
 - 23) Kanegane H, Futatani T, Wang Y, et al : Clinical and mutational characteristics of X-linked agammaglobulinemia and its carrier identified by flow cytometric assessment combined with genetic analysis. *J Allergy Clin Immunol* **108** : 1012-1020, 2001
 - 24) Shinozaki K, Kanegane H, Matsukura H, et al : Activation-dependent T cell expression of the X-linked lymphoproliferative disease gene product SLAM-associated protein and its assessment for patient detection. *Int Immunol* **14** : 1215-1223, 2002

成人型分類不能型免疫不全症の診断基準・診断方法の確立
及び治療方法の開発に関する研究

厚生労働科学研究費補助金 難治性疾患克服研究事業
平成 22 年度～平成 23 年度 総合研究報告書

研究代表者 森尾 友宏
東京医科歯科大学大学院医歯学総合研究科発生発達病態学分野
発行 平成 24 年 3 月
印刷 富沢印刷株式会社

